

## Large magnetocaloric effects of RFeSi (R=Tb and Dy) compounds for magnetic refrigeration in nitrogen and natural gas liquefaction

H. Zhang, Y. J. Sun, E. Niu, L. H. Yang, J. Shen et al.

Citation: *Appl. Phys. Lett.* **103**, 202412 (2013); doi: 10.1063/1.4832218

View online: <http://dx.doi.org/10.1063/1.4832218>

View Table of Contents: <http://apl.aip.org/resource/1/APPLAB/v103/i20>

Published by the *AIP Publishing LLC*.

---

### Additional information on Appl. Phys. Lett.

Journal Homepage: <http://apl.aip.org/>

Journal Information: [http://apl.aip.org/about/about\\_the\\_journal](http://apl.aip.org/about/about_the_journal)

Top downloads: [http://apl.aip.org/features/most\\_downloaded](http://apl.aip.org/features/most_downloaded)

Information for Authors: <http://apl.aip.org/authors>



[www.goodfellowusa.com](http://www.goodfellowusa.com)

**Goodfellow**

metals • ceramics • polymers  
composites • compounds • glasses

**Save 5% • Buy online**

**70,000 products • Fast shipping**

# Large magnetocaloric effects of $R\text{FeSi}$ ( $R = \text{Tb}$ and $\text{Dy}$ ) compounds for magnetic refrigeration in nitrogen and natural gas liquefaction

H. Zhang,<sup>1,a)</sup> Y. J. Sun,<sup>1</sup> E. Niu,<sup>2,3</sup> L. H. Yang,<sup>1,2</sup> J. Shen,<sup>4</sup> F. X. Hu,<sup>2</sup> J. R. Sun,<sup>2</sup> and B. G. Shen<sup>2</sup>

<sup>1</sup>*School of Materials Science and Engineering, University of Science and Technology of Beijing, Beijing 100083, People's Republic of China*

<sup>2</sup>*State Key Laboratory for Magnetism, Institute of Physics, Chinese Academy of Sciences, Beijing 100190, People's Republic of China*

<sup>3</sup>*Beijing Zhong ke San Huan Research, No.10 Chuangxin Rd., Changping District, Beijing 102200, People's Republic of China*

<sup>4</sup>*Key laboratory of Cryogenics, Technical Institute of Physics and Chemistry, Chinese Academy of Sciences, Beijing 100190, People's Republic of China*

(Received 5 June 2013; accepted 5 November 2013; published online 15 November 2013)

Magnetic properties and magnetocaloric effect (MCE) of intermetallic  $R\text{FeSi}$  ( $R = \text{Tb}$  and  $\text{Dy}$ ) compounds have been investigated systematically. The  $R\text{FeSi}$  compounds undergo a second-order magnetic transition from ferromagnetic to paramagnetic states with the variation of temperature. The Curie temperatures determined from magnetization measurements are 110 K and 70 K for  $\text{TbFeSi}$  and  $\text{DyFeSi}$ , respectively, which are quite close to the liquefaction temperatures of natural gas (111 K) and nitrogen (77 K). Both compounds exhibit nearly same large MCE around their respective ordering temperatures. For a low magnetic field change of 1 T, the maximum values of magnetic entropy change  $-\Delta S_M$  and adiabatic temperature change  $\Delta T_{ad}$  are 5.3 J/kg K and 2.1 K for  $\text{TbFeSi}$ , 4.8 J/kg K and 1.7 K for  $\text{DyFeSi}$ , respectively. Furthermore, a composite material based on  $(\text{Tb}_{1-x}\text{Dy}_x)\text{FeSi}$  compounds is designed theoretically by using a numerical method, and it exhibits a constant  $-\Delta S_{com}$  of  $\sim 1.4$  J/kg K for a field change of 1 T in the wide temperature range of 67–108 K, satisfying the requirement of Ericsson-cycle magnetic refrigeration over the liquefaction temperatures of nitrogen and natural gas. © 2013 AIP Publishing LLC. [<http://dx.doi.org/10.1063/1.4832218>]

Recently, magnetic refrigeration based on magnetocaloric effect (MCE) has emerged as one of the most promising technologies due to its various advantages in comparison with conventional vapor-compression refrigeration.<sup>1,2</sup> In addition to room-temperature magnetocaloric materials, much attention has also been paid to the materials with large MCE at low temperature due to their potential applications in refrigeration for gas liquefaction.<sup>3,4</sup> Therefore, it is of importance to exploit magnetic refrigerants that exhibit large MCE especially around the liquefaction temperatures of nitrogen (77 K) and natural gas (111 K). In response to the variation of magnetic field, the magnitude of MCE can be characterized by magnetic entropy change ( $\Delta S_M$ ) and/or adiabatic temperature change ( $\Delta T_{ad}$ ).<sup>5,6</sup> Besides, refrigerant capacity ( $RC$ ) has been considered as another important criterion to quantify the heat transferred in the thermodynamic cycle. It has been found that many materials with first-order phase transition (FOPT) exhibit large  $\Delta S_M$  and  $\Delta T_{ad}$  around the transition temperature.<sup>7–9</sup> However, FOPT is often accompanied by considerable thermal and magnetic hystereses, which always reduce the effective  $RC$ .<sup>10,11</sup> In contrast, many second-order phase transition (SOPT) materials present reversible MCE and large  $RC$  over a broad temperature region.<sup>12,13</sup> In addition, it is known that the maximum field supplied by a permanent magnet is usually lower than 2 T.

Therefore, it is preferable to develop magnetocaloric materials with SOPT which exhibit large reversible MCE under low magnetic field change (e.g., 1 T).

Magnetic refrigeration systems based on Ericsson cycle, which consists of two isothermal and two isofield steps, have been considered to be quite suitable to real refrigeration applications.<sup>14,15</sup> Thermodynamic analysis shows that an ideal Ericsson cycle requires constant  $\Delta S_M$  as a function of temperature over the operating temperature range.<sup>5</sup> This condition is difficult to be satisfied by single magnetocaloric material, in which  $\Delta S_M$  falls off rapidly away from the transition temperature. In contrast, composite magnetic materials have been considered as the most promising choice to accomplish the requirement of Ericsson cycle since composites can lead to almost constant  $\Delta S_M$  over an enlarged temperature span.<sup>3,16</sup> In this context, a series of materials with varying transition temperatures and similar  $\Delta S_M$  are desirable for the design of composite magnetocaloric materials.<sup>17</sup>

In previous studies, we found that  $\text{ErFeSi}$  exhibits a large reversible MCE around 22 K under relatively low magnetic field change (i.e., 2 T), suggesting  $\text{ErFeSi}$  as the attractive candidate for magnetic refrigerants around liquid hydrogen temperature.<sup>4</sup> In this letter, we further report the magnetic properties and MCE of  $R\text{FeSi}$  ( $R = \text{Tb}$  and  $\text{Dy}$ ) compounds.

The  $R\text{FeSi}$  ( $R = \text{Tb}$  and  $\text{Dy}$ ) were synthesized by arc-melting appropriate proportion of constituent components in a water-cooled copper hearth under purified argon atmosphere.

<sup>a)</sup> Author to whom correspondence should be addressed. E-mail address: zhanghuxt@gmail.com. Tel.: +86-10-62334807. Fax: +86-10-82649485.

The purities of constituent elements are better than 99.9 wt.% with major impurities, given as wt. ppm, as follows: Tb (O < 300, Fe < 200, Si < 100), Dy (O < 200, Fe < 200, Si < 100), Fe (O < 56, Ca < 19, Ni < 12), and Si (Fe < 200, Al < 200, Ca < 10). The obtained ingots (~10 g in the shape of button) were sealed in a high-vacuum quartz tube, annealed at 1373 K for 35 days, and then quenched into liquid nitrogen. Powder X-ray diffraction (XRD) measurements were performed at room temperature by using Cu  $K\alpha$  radiation. The Rietveld refinements based on XRD patterns confirm that both samples crystallize in a single phase with tetragonal CeFeSi-type structure (space group  $P4/nmm$ ), and the lattice parameters are  $a = 3.986(5)$  Å and  $c = 6.777(7)$  Å for TbFeSi,  $a = 3.968(4)$  Å and  $c = 6.762(6)$  Å for DyFeSi, respectively.<sup>18</sup> These results are in a good agreement with the values in earlier reports.<sup>19,20</sup> Magnetizations were measured by employing a MPMS SQUID VSM magnetometer from Quantum Design Inc, and the samples are small particles of 1.83 and 2.42 mg for TbFeSi and DyFeSi, respectively. The specific heat capacities were measured by using a physical property measurement system (PPMS) from Quantum Design Inc, and the samples are 9.82 and 10.48 mg in the shape of thin slice for TbFeSi and DyFeSi, respectively.

The temperature ( $T$ ) dependences of zero-field-cooling (ZFC) and field-cooling (FC) magnetizations ( $M$ ) were measured in 0.05 T as shown in Fig. 1(a). These compounds undergo a ferromagnetic (FM) to paramagnetic (PM) transition, and the Curie temperatures ( $T_C$ ), corresponding to the peak of  $dM/dT$ - $T$  curve (inset (a1) of Fig. 1(a)), are 110 K and 70 K for TbFeSi and DyFeSi, respectively. The  $T_C$  values in this work are much different from the results in Ref. 20. In order to confirm the results, several  $R$ FeSi ( $R = \text{Tb}$  and  $\text{Dy}$ ) compounds were prepared in the same way as described above, and it turned out that all samples with same composition exhibit the same transition temperatures. We assume that the large difference of  $T_C$ s may be mainly caused by the different heat treatment techniques (2 weeks at 1173 K in Ref. 20), which might influence the homogeneity of samples and result in different compositions of matrix phases. In addition, these  $T_C$ s are quite close to the liquefaction temperatures of nitrogen (77 K) and natural gas (111 K), indicating the potential applications of  $R$ FeSi ( $R = \text{Tb}$  and  $\text{Dy}$ ) in these temperature ranges. An unusual discrepancy between ZFC and FC curves can be observed in PM state (inset (a2) of Fig. 1(a)), suggesting the existence of short-range FM correlations just above  $T_C$ .<sup>21,22</sup> Fig. 1(b) displays the  $M$ - $T$  curves for TbFeSi in various magnetic fields. It is clearly seen that the magnetization enhances with increasing magnetic field. Meanwhile, the increase of magnetic field also results in a slow magnetic transition and a slight increase of  $T_C$  from 110 K at 0.05 T to 115 K at 5 T, corresponding to the typical behavior of FM-PM transition.<sup>23</sup> Similar phenomenon is also observed in DyFeSi. The temperature dependence of the inverse dc susceptibilities ( $\chi^{-1}$ ) in 1 T and the Curie-Weiss fit for  $R$ FeSi are presented in the inset of Fig. 1(b). Above their respective ordering temperatures, the magnetic susceptibilities obey the Curie-Weiss law. The values of PM Curie temperature ( $\theta_P$ ) and effective magnetic moment ( $\mu_{\text{eff}}$ ) are  $\theta_P = 90$  K and  $\mu_{\text{eff}} = 10.28 \mu_B$  for TbFeSi,  $\theta_P = 69$  K and  $\mu_{\text{eff}} = 11.41 \mu_B$  for DyFeSi, respectively. The  $\mu_{\text{eff}}$  values are close to the free ion

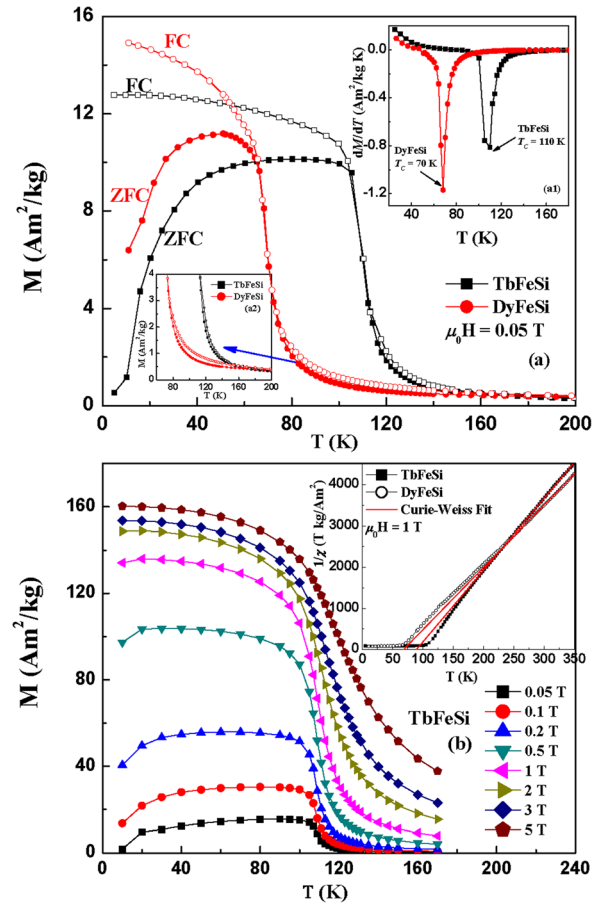


FIG. 1. (a) Temperature dependences of ZFC and FC magnetizations for  $R$ FeSi ( $R = \text{Tb}$  and  $\text{Dy}$ ) in 0.05 T in the temperature range from 5 K to 200 K. The inset (a1) shows the  $dM/dT$ - $T$  curves for these compounds. The inset (a2) shows a close view of the  $M$ - $T$  curves in the PM state. (b) Temperature dependences of magnetization for TbFeSi in various magnetic fields. The inset shows the temperature variation of inverse dc susceptibility ( $\chi^{-1}$ ) fitted to the Curie-Weiss law at 1 T in the temperature range of 5–350 K.

moments of  $\text{Tb}^{3+}$  ( $9.72 \mu_B$ ) and  $\text{Dy}^{3+}$  ( $10.63 \mu_B$ ), implying the absence of localized magnetic moment on Fe atoms in  $R$ FeSi.<sup>20</sup>

Figure 2 shows the magnetization isotherms of  $R$ FeSi ( $R = \text{Tb}$  and  $\text{Dy}$ ). The magnetization below  $T_C$  increases rapidly at low fields and tends to saturate with increasing field, indicating the typical FM behavior. At temperatures well above  $T_C$ , the magnetization isotherms show strong curvatures at low fields, confirming the presence of short-range FM correlations above  $T_C$ .<sup>24,25</sup> To investigate the magnetic reversibility, the  $M$ - $H$  curves of  $R$ FeSi around their respective  $T_C$  were measured in field increasing and decreasing modes. No magnetic hysteresis is observed in these isotherms, indicating the perfect reversibility of magnetic transitions. Furthermore, the Arrott plots (not shown here) of both compounds show positive slopes around  $T_C$ , proving the characteristic of second-order magnetic transition.<sup>26</sup> In addition, it is also found that the  $T_C$  values, determined from Arrott plots,<sup>27,28</sup> are 110 and 69.6 K for TbFeSi and DyFeSi, respectively, which are in a great agreement with the values from thermomagnetic curves.

The heat capacity ( $C_P$ ) curves for  $R$ FeSi ( $R = \text{Tb}$  and  $\text{Dy}$ ) in 0 and 2 T are presented in Fig. 3. The distinct  $\lambda$ -type



peaks in 0 T are observed around 105 K and 66 K for TbFeSi and DyFeSi, respectively, corresponding to the SOPT as observed in magnetic measurements. The peaks at their respective  $T_C$  are gradually broadened and suppressed with the increase of magnetic field, suggesting the typical characteristic of ferromagnet.<sup>4,5</sup> The presence of heat capacity peak is caused by the heat absorption during phase transition, which is utilized in randomization of magnetic moments around  $T_C$ . When magnetic field is applied, the process of randomization of magnetic moments would spread out over a wide temperature range, and thus broadening the maximum peak.<sup>7,29</sup>

As mentioned before, the magnitude of MCE can be characterized by  $\Delta S_M$  and/or  $\Delta T_{ad}$ . It is well known that the  $\Delta S_M$  can be calculated either from the magnetization isotherms by using Maxwell relation  $\Delta S_M(T, H) = \int_0^H (\partial M / \partial T)_H dH$  or from the heat capacity by using the equation  $\Delta S_M(T) = \int_0^T [C_H(T) - C_0(T)] / T dT$ , respectively.<sup>30</sup> However, sometimes there is a large difference between the values from the two methods due to either false calculation of Maxwell relation in the vicinity of a FOPT or the poor contact between sample and measuring platform during heat capacity measurement.<sup>4,31</sup> Here, we choose Maxwell relation to calculate  $\Delta S_M$ , which is more widely used,<sup>8,32,33</sup> so that would be easy to compare our results with those of most others. Figure 4(a) shows the temperature dependence of  $\Delta S_M$  under different magnetic field changes. For comparison, the  $\Delta S_M$  values for a field change of 2 T were also calculated from heat capacity data and are shown

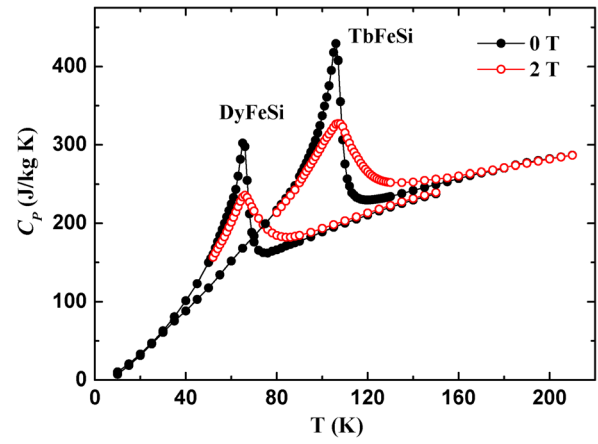


FIG. 3. Temperature dependence of heat capacities ( $C_p$ ) for RFeSi ( $R = \text{Tb}$  and  $\text{Dy}$ ) in 0 and 2 T. The temperature was changed in steps of 1 or 2 K in the vicinity of  $T_C$ , and it was in 5 K steps for temperature further away from  $T_C$ .

in Fig. 4(a). The results obtained from different methods are nearly consistent with each other as observed in other SOPT compounds.<sup>23,30</sup> For a field change of 1 T, the maximum  $-\Delta S_M$  values are 5.3 and 4.8 J/kg K for TbFeSi and DyFeSi, respectively. This large MCE under low field change is preferable to practical applications since the magnetic field of 1 T can be supplied by a permanent magnet.

As the most important criterion to evaluate MCE of magnetic refrigerants, the  $\Delta T_{ad}$  was calculated by using the

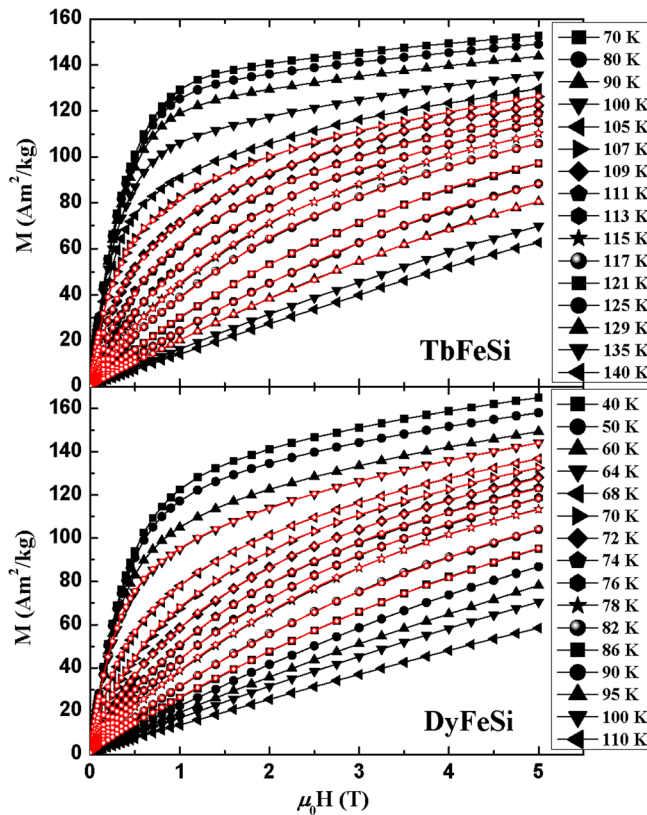


FIG. 2. Magnetization isotherms of RFeSi ( $R = \text{Tb}$  and  $\text{Dy}$ ) around their respective ordering temperatures. The magnetic field step was increased gradually, and it was 0.2 T when field is higher than 1 T. The temperature was changed in steps of 2 K in the vicinity of  $T_C$ , and it was in 4–10 K steps for temperature further away from  $T_C$ .

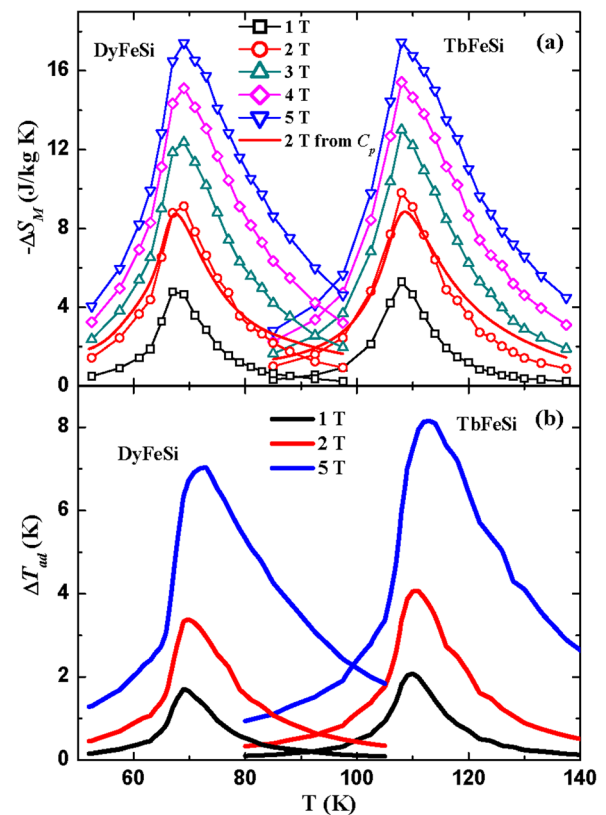


FIG. 4. (a) Temperature dependence of  $\Delta S_M$  for RFeSi ( $R = \text{Tb}$  and  $\text{Dy}$ ) under different magnetic field changes up to 5 T. The solid line indicates the  $\Delta S_M$  under a field change of 2 T calculated from heat capacity measurements. (b) Temperature dependence of  $\Delta T_{ad}$  for RFeSi ( $R = \text{Tb}$  and  $\text{Dy}$ ) under the magnetic field changes of 1, 2, and 5 T, respectively.

TABLE I. The ordering temperature  $T_{ord}$ , the magnetic entropy change  $\Delta S_M$ , and adiabatic temperature change  $\Delta T_{ad}$  for  $R\text{FeSi}$  ( $R = \text{Tb}$  and  $\text{Dy}$ ) and some other refrigerant materials with a magnetic ordering temperature in the similar temperature range.

Materials	$T_{ord}$ (K)	$-\Delta S_M$ (J/kg K)		$\Delta T_{ad}$ (K)		Refs.
		2 T	5 T	2 T	5 T	
NdFeAl	110	3.0	5.7	-	-	32
Tb <sub>5</sub> Si <sub>2</sub> Ge <sub>2</sub>	101	6.2	15.1	2.2	5.4	36
TbAl <sub>2</sub>	108	7.5	11.4	2.2	4.4	37
TbFeSi	110	9.8	17.5	4.1	8.2	This work
TbCoAl	70	5.3	10.5	-	-	33
Ho <sub>5</sub> Si <sub>4</sub>	76	6.6	14.8	2.6	6.1	38
EuO	69	8.5	17.5	3.2	6.8	23
DyFeSi	70	9.2	17.4	3.4	7.1	This work

equation  $\Delta T_{ad} = -\Delta S(T, H) \times T / C_P(T, H_0)$ , where  $C_P(T, H_0)$  is zero-field heat capacity. Figure 4(b) shows the temperature dependence of  $\Delta T_{ad}$  under different magnetic field changes. The maximum  $\Delta T_{ad}$  values under a field change of 1 T are 2.1 and 1.7 K for TbFeSi and DyFeSi, respectively. In order to get a better comparison of MCE, the MCE of  $R\text{FeSi}$  and some other refrigerant materials with similar magnetic transition temperatures are listed in Table I. It can be seen that the MCEs of  $R\text{FeSi}$  ( $R = \text{Tb}$  and  $\text{Dy}$ ) are comparable with those of other materials in the similar temperature range, suggesting the applicability of these compounds around the liquefaction temperatures of nitrogen and natural gas.

Another feature worth noticing is the nearly same magnitude of MCE for TbFeSi and DyFeSi. As mentioned before, an ideal Ericsson cycle requires constant  $\Delta S_M$  over a large temperature range.<sup>5</sup> Considering the same crystal structure with similar lattice parameters for TbFeSi and DyFeSi, it is easy to expect that a series of  $(\text{Tb}_{1-x}\text{Dy}_x)\text{FeSi}$  compounds with different ordering temperatures but similar magnitude of  $\Delta S_M$  could be prepared to fulfill the required conditions.<sup>17,34</sup> Assuming that (1) the  $T_C$  of  $(\text{Tb}_{1-x}\text{Dy}_x)\text{FeSi}$  varies with respect to the de Gennes factor,<sup>34</sup> and (2) there is no interaction between  $\text{Tb}^{3+}$  and  $\text{Dy}^{3+}$  ions,<sup>17</sup> the values of  $T_C$  and  $\Delta S_M$  for  $(\text{Tb}_{1-x}\text{Dy}_x)\text{FeSi}$  can be estimated theoretically by using following equations:

$$T_C = (1-x)T_{C_{\text{Tb}}} + xT_{C_{\text{Dy}}}, \quad (1)$$

$$\begin{aligned} \Delta S(T, H) = & (1-x)\Delta S_{\text{Tb}}(T_{C_{\text{Tb}}} + \Delta T, H) \\ & + x\Delta S_{\text{Dy}}(T_{C_{\text{Dy}}} + \Delta T, H), \end{aligned} \quad (2)$$

where  $T_{C_{\text{Tb}}}$  and  $\Delta S_{\text{Tb}}$  are the  $T_C$  and  $\Delta S_M$  for TbFeSi,  $T_{C_{\text{Dy}}}$  and  $\Delta S_{\text{Dy}}$  are the  $T_C$  and  $\Delta S_M$  for DyFeSi, and  $\Delta T = T - T_C$ . Figure 5 shows the temperature dependence of calculated  $\Delta S_M$  for  $(\text{Tb}_{1-x}\text{Dy}_x)\text{FeSi}$  under a field change of 1 T. This series of compounds exhibit nearly same  $\Delta S_M$  peaks from 67 to 108 K. Based on these compounds, a composite material can be formed and the optimum mass ratio  $y_i$  of each component, determined by using a numerical method,<sup>16</sup> is as follows:  $y_1 = 19.43$  wt. %,  $y_2 = 13.32$  wt. %,  $y_3 = 13.47$  wt. %,  $y_4 = 13.74$  wt. %,  $y_5 = 15.08$  wt. %, and

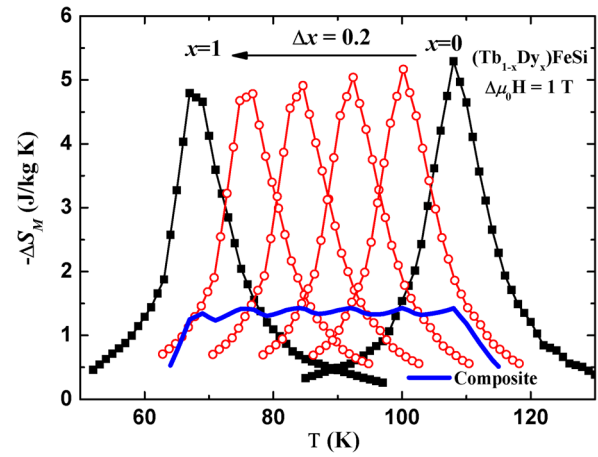


FIG. 5. Temperature dependence of calculated  $\Delta S_M$  for  $(\text{Tb}_{1-x}\text{Dy}_x)\text{FeSi}$  ( $x = 0-1$ ) compounds and the composite material under a magnetic field change of 1 T.

$y_6 = 24.96$  wt. % for  $x = 0, 0.2, 0.4, 0.6, 0.8$ , and  $1.0$ , respectively. The magnetic entropy change of this composite can be estimated by using the equation  $\Delta S_{\text{com}} = \sum_{i=1}^6 y_i \Delta S_i$  and is shown in Fig. 5. It is seen that the composite exhibits a constant  $-\Delta S_{\text{com}}$  of  $\sim 1.4$  J/kg K in the wide temperature range. Besides, the RC value of composite, calculated by integrating numerically the area under the  $\Delta S_M$ - $T$  curve with defining the temperatures at half maximum of peak as the integration limits,<sup>35</sup> is 64 J/kg for a field change of 1 T, which is 49% and 64% higher than those of TbFeSi (43 J/kg) and DyFeSi (39 J/kg). This result suggests that the composite can be a good candidate of magnetic refrigerants for Ericsson cycle in the temperature range of 67–108 K.

In summary, TbFeSi and DyFeSi show a second-order FM-PM transition around  $T_C = 110$  K and 70 K, respectively. No magnetic hysteresis is observed in both compounds, suggesting the perfect reversibility of magnetic transitions. The maximum values of  $-\Delta S_M$  and  $\Delta T_{ad}$  under a low field change of 1 T are 5.3 J/kg K and 2.1 K for TbFeSi, 4.8 J/kg K and 1.7 K for DyFeSi, respectively. Moreover, theoretical analysis suggests that a series of  $(\text{Tb}_{1-x}\text{Dy}_x)\text{FeSi}$  compounds may exhibit similar  $\Delta S_M$  in a wide temperature range, and then a composite material based on these compounds is proposed to work for magnetic refrigeration with Ericsson cycle over the liquefaction temperatures of nitrogen and natural gas.

This work was supported by the National Natural Science Foundation of China (Grant Nos. 51001114, 11274357, 51271196, 51021061, 51271192, and 11004204), the Hi-Tech Research and Development program of China (No. 2011AA03A404), the Key Research Program of the Chinese Academy of Sciences, the National Basic Research Program of China (No. 2010CB833102), and the Fundamental Research Funds for the Central Universities (No. FRF-TP-13-007 A).

<sup>1</sup>C. B. Zimm, A. Jastrab, A. Sternberg, V. K. Pecharsky, K. A. Gschneidner, Jr., M. Osborne, and I. Anderson, Adv. Cryog. Eng. **43**, 1759 (1998).

<sup>2</sup>K. A. Gschneidner, Jr., V. K. Pecharsky, and A. O. Tsokol, Rep. Prog. Phys. **68**, 1479 (2005).

- <sup>3</sup>A. Chaturvedi, S. Stefanoski, M. H. Phan, G. S. Nolas, and H. Srikanth, *Appl. Phys. Lett.* **99**, 162513 (2011).
- <sup>4</sup>H. Zhang, B. G. Shen, Z. Y. Xu, J. Shen, F. X. Hu, J. R. Sun, and Y. Long, *Appl. Phys. Lett.* **102**, 092401 (2013).
- <sup>5</sup>A. M. Tishin and Y. I. Spichkin, in *The Magnetocaloric Effect and its Applications*, edited by J. M. D. Coey, D. R. Tilley, and D. R. Vij (IOP Publishing, Bristol, 2003).
- <sup>6</sup>V. I. Zverev, A. M. Tishin, and M. D. Kuz'min, *J. Appl. Phys.* **107**, 043907 (2010).
- <sup>7</sup>V. K. Pecharsky and K. A. Gschneidner, Jr., *Phys. Rev. Lett.* **78**, 4494 (1997).
- <sup>8</sup>O. Tegus, E. Brück, K. H. J. Buschow, and F. R. de Boer, *Nature* **415**, 150 (2002).
- <sup>9</sup>F. X. Hu, B. G. Shen, J. R. Sun, Z. H. Cheng, G. H. Rao, and X. X. Zhang, *Appl. Phys. Lett.* **78**, 3675 (2001).
- <sup>10</sup>V. Provenzano, A. J. Shapiro, and R. D. Shull, *Nature* **429**, 853 (2004).
- <sup>11</sup>H. Zhang, J. Shen, Z. Y. Xu, X. Q. Zheng, F. X. Hu, J. R. Sun, and B. G. Shen, *J. Magn. Magn. Mater.* **324**, 484 (2012).
- <sup>12</sup>L. W. Li, M. Kadonaga, D. X. Huo, Z. H. Qian, T. Namiki, and K. Nishimura, *Appl. Phys. Lett.* **101**, 122401 (2012).
- <sup>13</sup>H. Zhang, Z. Y. Xu, X. Q. Zheng, J. Shen, F. X. Hu, J. R. Sun, and B. G. Shen, *J. Appl. Phys.* **109**, 123926 (2011).
- <sup>14</sup>G. V. Brown, *J. Appl. Phys.* **47**, 3673 (1976).
- <sup>15</sup>J. R. Gomez, R. F. Garcia, A. D. Catoira, and M. R. Gomez, *Renewable Sustainable Energy Rev.* **17**, 74 (2013).
- <sup>16</sup>A. Smaili and R. Chahine, *J. Appl. Phys.* **81**, 824 (1997).
- <sup>17</sup>B. J. Korte, V. K. Pecharsky, and K. A. Gschneidner, Jr., *J. Appl. Phys.* **84**, 5677 (1998).
- <sup>18</sup>B. A. Hunter, *IUCR Comm. Powder Diffraction*, **20**, 21 (1998).
- <sup>19</sup>O. I. Bodak, E. I. Gladyshevskii, and P. I. Kripyakevich, *Zh. Strukt. Khim.* **11**, 283 (1970).
- <sup>20</sup>R. Welter, G. Venturini, and B. Malaman, *J. Alloys Compd.* **189**, 49 (1992).
- <sup>21</sup>Z. W. Ouyang, V. K. Pecharsky, K. A. Gschneidner, Jr., D. L. Schlagel, and T. A. Lograsso, *Phys. Rev. B* **74**, 094404 (2006).
- <sup>22</sup>H. Zhang, Ya. Mudryk, Q. Cao, V. K. Pecharsky, K. A. Gschneidner, Jr., and Y. Long, *J. Appl. Phys.* **107**, 013909 (2010).
- <sup>23</sup>K. Ahn, A. O. Pecharsky, J. K. A. Gschneidner, Jr., and V. K. Pecharsky, *J. Appl. Phys.* **97**, 063901 (2005).
- <sup>24</sup>R. Mallik, E. V. Sampathkumaran, and P. L. Paulose, *Solid State Commun.* **106**, 169 (1998).
- <sup>25</sup>N. K. Singh, K. G. Suresh, R. Nirmala, A. K. Nigam, and S. K. Malik, *J. Appl. Phys.* **101**, 093904 (2007).
- <sup>26</sup>B. K. Banerjee, *Phys. Lett.* **12**, 16 (1964).
- <sup>27</sup>A. Arrott, *Phys. Rev.* **108**, 1394 (1957).
- <sup>28</sup>V. I. Zverev, R. R. Gimaev, A. M. Tishin, Ya. Mudryk, K. A. Gschneidner, Jr., and V. K. Pecharsky, *J. Magn. Magn. Mater.* **323**, 2453 (2011).
- <sup>29</sup>N. K. Singh, K. G. Suresh, A. K. Nigam, and S. K. Malik, *J. Appl. Phys.* **97**, 10A301 (2005).
- <sup>30</sup>V. K. Pecharsky and K. A. Gschneidner, Jr., *J. Appl. Phys.* **86**, 565 (1999).
- <sup>31</sup>J. D. Zou, B. G. Shen, B. Gao, J. Shen, and J. R. Sun, *Adv. Mater.* **21**, 693 (2009).
- <sup>32</sup>L. Si, J. Ding, L. Wang, Y. Li, H. Tan, and B. Yao, *J. Alloys Compd.* **316**, 260 (2001).
- <sup>33</sup>X. X. Zhang, F. W. Wang, and G. H. Wen, *J. Phys.: Condens. Matter* **13**, L747 (2001).
- <sup>34</sup>H. Zhang, Z. Y. Xu, X. Q. Zheng, J. Shen, F. X. Hu, J. R. Sun, and B. G. Shen, *Solid State Commun.* **152**, 1734 (2012).
- <sup>35</sup>K. A. Gschneidner, Jr., V. K. Pecharsky, A. O. Pecharsky, and C. B. Zimm, *Mater. Sci. Forum* **315-317**, 69 (1999).
- <sup>36</sup>H. Huang, A. O. Pecharsky, V. K. Pecharsky, and K. A. Gschneidner, Jr., *Adv. Cryog. Eng.* **48**, 11 (2002).
- <sup>37</sup>M. I. Ilyn, A. M. Tishin, V. K. Pecharsky, A. O. Pecharsky, and K. A. Gschneidner, Jr., *CEC/ICMC* (Madison, 2001).
- <sup>38</sup>N. K. Singh, D. Paudyal, V. K. Pecharsky, and K. A. Gschneidner, Jr., *J. Appl. Phys.* **107**, 09A921 (2010).